Identification of Novel *RPGR* ORF15 Mutations in X-linked Progressive Cone-Rod Dystrophy (XLCORD) Families

Neil D. Ebenezer,[1,2] *Michel Michaelides,*[1,2,3] *Sharon A. Jenkins,*[3] *Isabelle Audo,*[3] *Andrew R. Webster,*[1,3] *Michael E. Cheetham,*[4] *Andrew Stockman,*[5] *Eamonn R. Maher,*[6] *John R. Ainsworth,*[7] *John R. Yates,*[8] *Keith Bradshaw,*[9] *Graham E. Holder,*[4] *Anthony T. Moore,*[1,3] *and Alison J. Hardcastle*[1]

Purpose. To test the incidence of mutations in *RPGR* ORF15 in six families with X-linked progressive retinal degeneration (cone-rod dystrophy [XLCORD], macular or cone dystrophy) and to undertake a detailed phenotypic assessment of families in whom ORF15 mutations were identified.

Methods. To amplify and sequence ORF15 in its entirety, a cloning strategy was developed. Families with mutations in ORF15 underwent electrophysiological testing, color vision assessment, color fundus photography, and fundus autofluorescence (AF) imaging.

Results. Novel protein truncation mutations were identified in two families. In family A, a 2-bp mutation was identified in ORF15+A1094C G1095T, predicted to result in a truncated protein (E364D/E365X). In family B, a G-to-T transversion (ORF15+1176G>T) resulted in a nonsense mutation (G392X). Characteristics of phenotype in both families included progressive deterioration of central vision and subsequently night vision, mild photophobia, and moderate to high myopia. Ophthalmoscopic abnormalities were generally confined to the macula. A parafoveal ring of increased AF was observed, and electrophysiological evidence of a greater generalized abnormality in cone than rod responses were consistent with a cone–rod dystrophy phenotype.

Conclusions. The cloning strategy for ORF15 facilitated comprehensive sequence analysis in patients. Two families were identified with nonsense mutations, and clinical evaluation revealed them both to have a similar phenotype. The presence of a parafoveal ring of increased AF was an early indicator of affected status in these families. No disease-causing mutations in ORF15 were detected in four other families, suggesting that ORF15 mutations may not be the most common cause of XLCORD. (*Invest Ophthalmol Vis Sci.* 2005;46:1891–1898) DOI:10.1167/iovs.04-1482

Mutations in the retinitis pigmentosa GTPase regulator (*RPGR*) gene are a major cause of X-linked retinitis pigmentosa (XLRP).[1–12] XLRP is a severe form of RP in which affected males are symptomatic from early childhood. Most affected males are myopic, having night blindness in the first decade followed by peripheral field loss, and finally central vision loss. Most patients are blind by the end of the third decade. Female carriers display a broad spectrum of fundus appearances, ranging from normal to extensive retinal degeneration.[13,14]

X-linked cone–rod dystrophy (XLCORD) is a progressive disorder in which cone degeneration is greater than rod degeneration and usually involves the macula. Three chromosomal loci for XLCORD have been identified to date: *CORDX1* (Xp21.1-11.4; OMIM 304020), *CORDX2* (Xq27.2-28; OMIM; 300085), and *CORDX3* (Xp 11.4-q13.1; OMIM 300476).[15–17] Affected males have reduced visual acuity, variable photophobia, and color vision disturbance. Myopic refractive errors are common. In contrast to XLRP, full-field electroretinography (ffERG) shows a greater abnormality of cone responses than rod in the early stages of the disease.[15,18–20]

A new exon of *RPGR*, ORF15, has been identified as a mutation hotspot for XLRP.[3,9,11,12] More recently, mutations in ORF15 have also been identified in subjects with XLCORD and in a pedigree with X-linked recessive atrophic macular degeneration.[12,21–23] Four different ORF15 frameshift insertions and deletions, and one nonsense mutation have been described as a cause of XLCORD,[12,21,22] and an ORF15 nonsense mutation was described as a cause of X-linked macular degeneration (although several affected males in this pedigree had abnormal cone and rod ffERGs).[23]

The purpose of this study was to identify families with X-linked cone, cone–rod, or macular dystrophy; determine the contribution and distribution of ORF15 mutations; and characterize the phenotype in those patients in whom an ORF15 mutation was identified.

Patients and Methods

Families

Six British families with X-linked retinal dystrophy primarily affecting cone photoreceptors (cone, cone–rod, and macular dystrophy pheno-

From the Divisions of [1]Molecular Genetics, [4]Pathology, and [5]Visual Science, Institute of Ophthalmology, University College London, United Kingdom; [3]Moorfields Eye Hospital, London, United Kingdom; the [6]Section of Medical and Molecular Genetics, Department of Paediatrics and Child Health, University of Birmingham, The Medical School, Birmingham, United Kingdom; [7]Birmingham Midlands Eye Hospital and Birmingham Children's Hospital, Birmingham, United Kingdom; the [8]Department of Medical Genetics, University of Cambridge, Cambridge, United Kingdom; and the [9]Department of Ophthalmology, Addenbrookes Hospital, Cambridge, United Kingdom.

[2]Contributed equally to the work and therefore should be considered equivalent authors.

Supported by Grant 065454/Z/01/Z from the Wellcome Trust, the British Retinitis Pigmentosa Society, and the Guide Dogs for the Blind Association.

Submitted for publication December 16, 2004; revised February 7, 2005; accepted February 28, 2005.

Disclosure: **N.D. Ebenezer**, None; **M. Michaelides**, None; **S.A. Jenkins**, None; **I. Audo**, None; **A.R. Webster**, None; **M.E. Cheetham**, None; **A. Stockman**, None; **E.R. Maher**, None; **J.R. Ainsworth**, None; **J.R. Yates**, None; **K. Bradshaw**, None; **G.E. Holder**, None; **A.T. Moore**, None; **A.J. Hardcastle**, None

The publication costs of this article were defrayed in part by page charge payment. This article must therefore be marked "*advertisement*" in accordance with 18 U.S.C. §1734 solely to indicate this fact.

Corresponding author: Alison J. Hardcastle, Division of Molecular Genetics, Institute of Ophthalmology, University College London, London EC1V 9EL, UK; a.hardcastle@ucl.ac.uk.

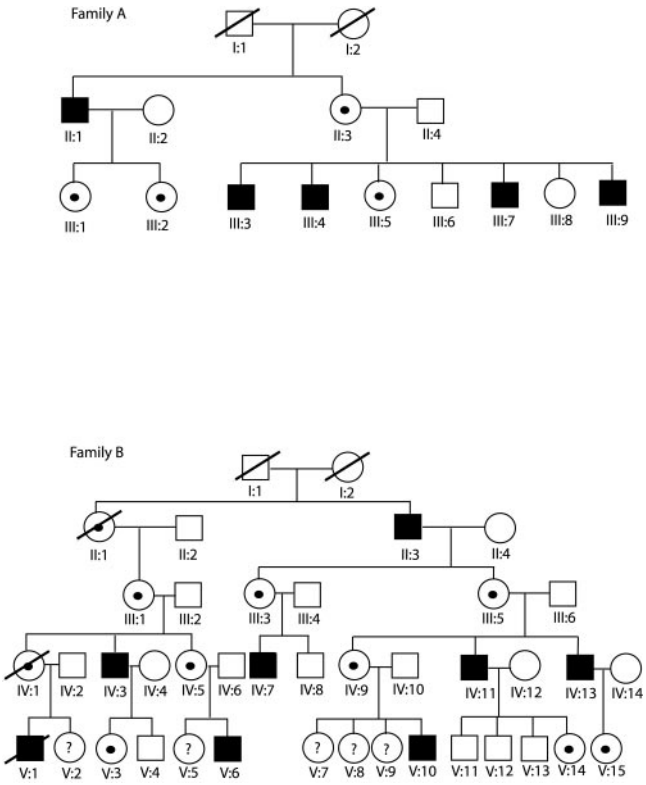

FIGURE 1. Abridged pedigree structure for X-linked cone–rod dystrophy family A and family B. *Circles*: females; *squares*: males; *open symbols*: unaffected; *filled symbols*: affected; *dot*: female carrier; *question mark*: female with status undefined.

types) were ascertained. After informed consent was obtained, blood samples from affected and unaffected family members were taken for DNA extraction and subsequent mutation screening of *RPGR*. Detailed phenotyping was performed in the two families (families A and B; Fig. 1) in whom ORF15 mutations were identified. The protocol of the study adhered to the tenets of the Declaration of Helsinki and was approved by the local ethics committee.

Clinical Assessment of Patients

A full medical history was taken and ophthalmic examination performed. Subjects underwent color fundus photography and fundus autofluorescence (AF) imaging with a confocal scanning laser ophthalmoscope (cSLO; HRA, Heidelberg, Germany).

Electrophysiological assessment included an electro-oculogram (EOG), ffERG, and pattern (P)ERG, incorporating the protocols recommended by the International Society for Clinical Electrophysiology of Vision.[24–26] Color vision testing was performed using the Hardy, Rand, Ritter (HRR) plates (American Optical Company, New York, NY) and the Ishihara pseudoisochromatic plates. Female subjects underwent additional detailed psychophysical testing including red–green (Rayleigh equation) anomaloscope matches, and the Farnsworth Munsell (FM) 100-hue test. The FM 100-hue test was viewed under a desk lamp (6500K, Illuminant D-65, Sol-Source Daylight; Gretag MacBeth, New Windsor, NY). With these tests, it was possible to diagnose mild or severe red–green color vision deficiencies.

Strategy for Screening ORF15

The coding region of *RPGR* ORF15 was sequenced in its entirety by PCR amplification, cloning, and subsequent sequencing of the cloned product.

Genomic DNA was extracted from peripheral blood leukocytes (Nucleon BACC2 kit; Tepnel Life Sciences, Manchester, UK), and a single PCR product of 1786 bp was amplified with forward and reverse primers (ORF15F 5′-GTATGATTTTAAATGTGATCGCTTGTCAGAG-3′ and ORF15R 5′-AAGGCATTTAAATTGTCTGACTGGCCATAATC-3′) encompassing the entire open reading frame of 1706 bp. The following conditions were used: a 50 μL PCR reaction containing 100 ng of DNA, 1 μM of forward and reverse primers, 25 μL PCR mix (ReddyMix; AB-0795; ABgene, Epsom, UK); PCR amplification was performed with 1 cycle of 95°C for 5 minutes; 35 cycles of 95°C for 30 seconds, 56°C for 30 seconds, and 72°C for 1 minute 30 seconds; and 1 cycle of 72°C for 5 minutes. The resultant amplimer was purified through a column (Qiagen, Valencia, CA) and then cloned into the pGEM-Teasy vector, according to the manufacturer's recommendations (Promega, Madison, WI). The plasmid DNA was isolated (GenElute mini prep kit; Sigma-Aldrich, Poole, UK) and sequenced (model 3100; Applied Biosystems, Inc., [ABI], Foster City, CA) with M13 vector primers and ORF15-specific primers, to provide full bidirectional coverage of ORF15 (details of all primers used for sequencing are available on request). The sequencing reactions were performed with dye terminator chemistry (BigDye Terminator Cycle Sequencing, for the pyrimidine-rich strand and dGTP BigDye Terminator Cycle Sequencing, for the purine-rich strand; ABI).

Mutations identified were confirmed by a combination of independent cloning experiments, specific PCR amplification and direct sequencing of the mutated ORF15 fragment, and segregation with disease.

RESULTS

RPGR ORF15 Genotype

A bidirectional sequence contig was created for each sequence, by using M13 forward and reverse primers and internal sequencing primers within *RPGR* ORF15.

In family A, two consecutive substitutions were identified in ORF15+A1094C G1095T (Fig. 2A) that created a premature stop codon that was predicted to result in a truncated protein (E364D/E365X). In family B, a G-to-T transversion (ORF15+1176G>T; Fig. 2B) resulted in a nonsense mutation (G392X). Both of the changes identified are novel and are likely to result in a truncated protein. These sequence variations were therefore considered to be pathogenic mutations.

The mutations were confirmed by PCR amplification and direct sequencing of the mutated ORF15 fragment in other individuals from each family to demonstrate segregation with disease. The ORF15 mutations identified segregated uniquely in all affected subjects and carrier females tested in each family. These mutations were not detected in unaffected control chromosomes.

Clinical Assessment

Family A. Five affected males, three obligate carriers, and two nonobligate female members of a three-generation British family with X-linked retinal dystrophy were assessed (Fig. 1). Two affected males, III:7 and III:9, aged 40 and 37 years, respectively, admitted to mild photophobia and had myopia, but were otherwise asymptomatic. The remaining three affected males reported mild to moderate photophobia and reduced central and color vision. Onset of symptoms was in the fourth decade. All three reported that vision was better under mesopic conditions and that they experienced slow visual adaptation when moving from a dark to a bright environment. Nyctalopia was noted 5 to 10 years after the onset of reduced central visual function; nevertheless, all three symptomatic males reported that their night vision was better than that in daylight. All five affected males had moderate to high myopia with variable astigmatism. Visual acuity ranged between 6/5 and counting fingers. Color vision was absent in all the affected males. There was no evidence of nystagmus. Dilated fundoscopy revealed a range of age-dependent macular phenotypes, from mild changes at the level of the retinal pigment epithe-

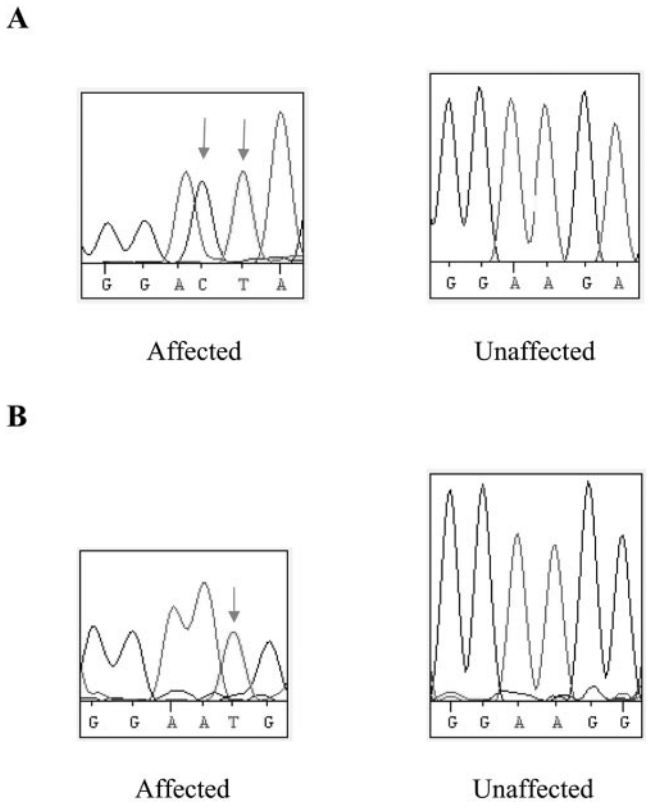

FIGURE 2. Representative electropherograms showing affected male mutations in ORF15. (**A**) Affected male ORF15 sequence from family A showing the mutation ORF15+A1094C G1095T, compared to an unaffected sequence. (**B**) Affected male ORF15 sequence for family B showing a G-to-T transversion (ORF15+1176G>T), compared with an unaffected sequence.

lium (RPE) to frank macular atrophy and pigmentation (Fig. 3). All male subjects had fundi consistent with significant myopia, with chorioretinal thinning, myopic optic discs, and peripapillary atrophy. Peripheral retinal examination findings were normal in all individuals, except II:1, the oldest affected male, who was found to have peripheral paving-stone retinal degeneration.

Asymptomatic individual III:9 did not have a definite macular disturbance on ophthalmoscopy, however autofluorescence (AF) imaging demonstrated a parafoveal ring of increased AF. All affected males had a parafoveal ring of increased AF of variable intensity and size (Fig. 3). Corresponding areas of decreased AF were evident in older subjects (II:1, III:3, and III:4) in whom macular atrophy was present. Electrophysiological testing demonstrated absent pattern and focal ERGs in all affected males, in keeping with severe bilateral macular dysfunction. ffERG showed cone ERGs to be more severely reduced than rod-specific ERGs in all male subjects, consistent with a cone–rod dystrophy phenotype. Representative electrophysiological traces are shown in Figure 4.

Five females were also assessed, of whom three (II:3, III:1, and III:2) were obligate carriers. The three obligate carriers (II:3, III:1, and III:2) and III:8 were asymptomatic. III:5, who was 50 years of age, reported a gradual deterioration in both central and night vision over the preceding 2 years, with VA recorded as 6/9 in both eyes. The other female subjects had excellent visual acuity, ranging between 6/4 and 6/5, except for II:3, who had a cataract in her right eye and an amblyopic left eye (6/9; 6/36). Color vision was normal in all subjects, with no evidence of pseudoprotanomaly[27] or other color vision deficiencies. The three obligate carriers and III:5 had a bilateral disturbance of the RPE located temporal to the macula (Fig. 3). These four subjects were found to carry the *RPGR* ORF15 mutation segregating in family A, suggesting that the ophthalmoscopically identified RPE mottling temporal to the macula signifies carrier status. Unlike the affected male subjects, the carrier females in this family displayed no abnormality on AF imaging. Individual III:8 does not carry the gene mutation. Peripheral retinal examination was normal in all individuals. Electrophysiological testing revealed variable retinal responses. III:1, III:2, and III:8 had normal PERGs and ffERGs. However, the two older individuals II:3 and III:5 were found to have abnormal retinal electrophysiology. Both II:3 (73 years of age), and III:5 (50 years of age) had bilaterally undetectable pattern and focal ERGs; the ffERG showed reduced responses with greater reduction in cone ERGs than rod-specific responses (Fig. 4). Clinical findings for this family are summarized in Table 1.

Family B. Five affected males and four obligate carriers of a five-generation British family with X-linked retinal dystrophy were assessed, and retrospective data were examined (Fig. 1). The five affected males had bilateral reduced central vision, with three of these subjects (IV:13, IV:11, and V:10) complaining of photophobia. Onset was between the second and fourth decades, with subsequent gradual deterioration of visual acuity and color vision. Two of the affected males (IV:11 and V:10) also reported nyctalopia, although individual V:10 (22 years of age) at the time of the study had normal rod responses. All the affected males had myopia with variable astigmatism, with the exception of V:10, who had hyperopia and astigmatism. Visual acuities ranged from 6/6 to counting fingers. None of the subjects had nystagmus, and color vision was absent in all affected male subjects. On fundus examination, the older affected males (IV:3, V:1, IV:13, and IV:11) showed variable degrees of macular RPE atrophy and chorioretinal degeneration, which was most prominent in the inferior retina (Fig. 3). The youngest affected male patient (V:10) had subtle bilateral foveal RPE mottling, with AF imaging revealing bilateral parafoveal rings of increased AF (Fig. 3). V:10 also had a bilateral inferior retinal sheen or tapetal reflex. IV:11 had also been noted to have a retinal sheen in the third decade of life. Recent AF imaging of IV:11 showed reduced AF corresponding to the macular atrophy seen ophthalmoscopically, with a surrounding ring of increased AF (Fig. 3).

Electrophysiological testing performed in three of the affected males (IV:3, V:1, and IV:13) revealed data consistent with a cone–rod dystrophy phenotype (Fig. 5). IV:11 (44 years of age) was severely affected and found to have only residual cone and rod responses on ffERG testing. His nephew, V:10 (22 years of age), had bilateral markedly reduced pattern ERGs, suggestive of bilateral severe macular dysfunction, with ffERG recordings demonstrated generalized loss of cone function with minimal evidence of rod system involvement, consistent with a diagnosis of cone dystrophy. Representative electrophysiological traces are shown in Figure 5.

Visual acuity of obligate female carriers ranged from 6/5 to counting fingers (obligate carrier III:3 age 70 years). One female carrier, V:14, had poor vision secondary to bilateral congenital cataracts. Female carriers in this family had been noted to have a golden tapetal reflex. Subject IV:9 had macular RPE atrophy in the left eye, associated with reduced vision. The eldest obligate carrier, III:3 (70 years of age), had more extensive macular, peripapillary, and peripheral retinal atrophic changes (Fig. 3), and AF imaging showed decreased macular AF. Electrophysiological testing was performed for individual III:3, which showed unilateral abnormal pattern and full-field responses (Fig. 5). Clinical findings in this family are summarized in Table 2.

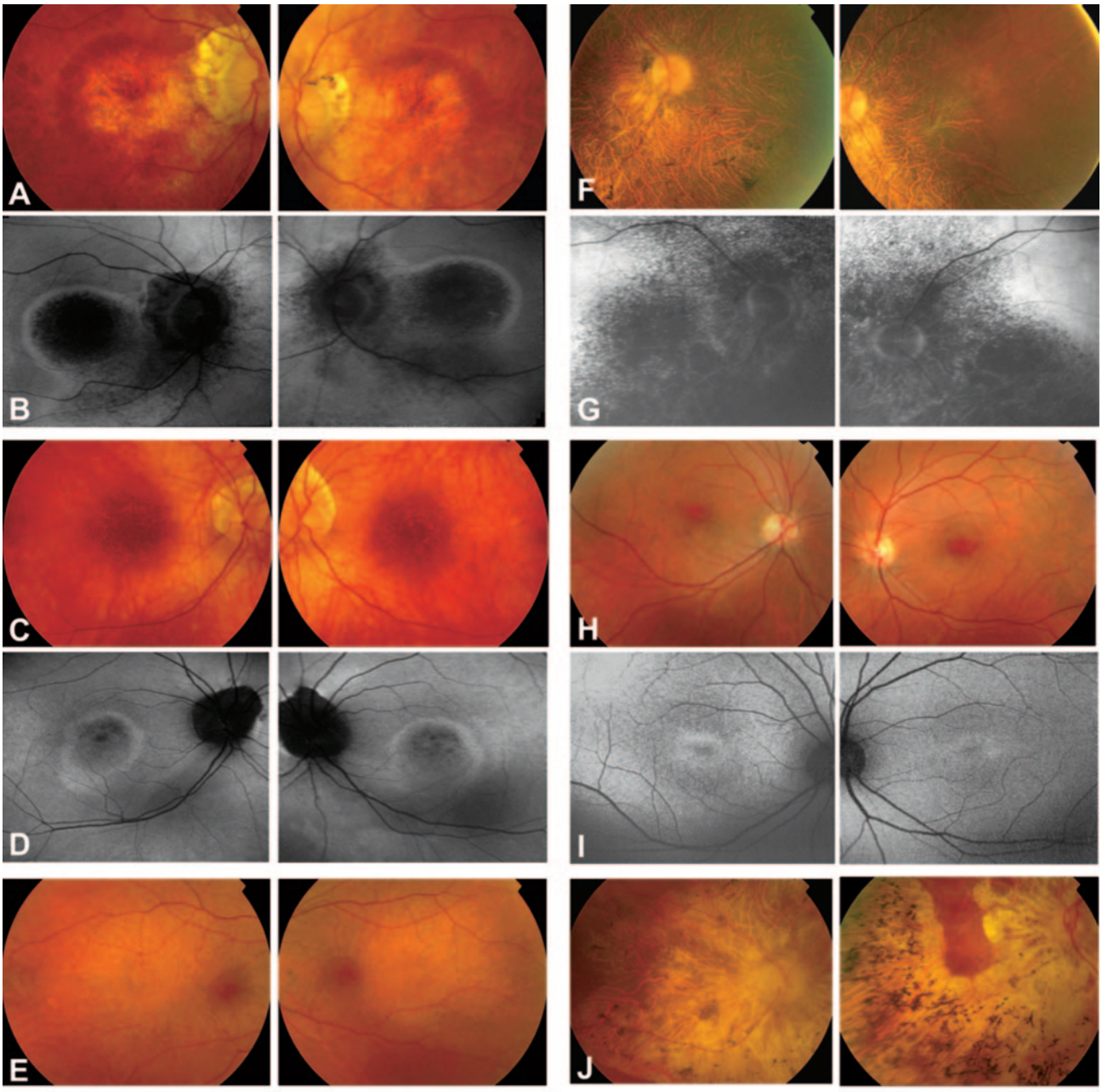

FIGURE 3. Fundus photographs and AF images of affected males and carrier females from families A and B. *Family A*, *patient III:4*: (**A**) Fundus photographs showing bilateral macular atrophy and pigmentation. Myopic chorioretinal degeneration with peripapillary atrophy can also be seen. (**B**) Fundus AF imaging showing bilateral markedly reduced macular AF, corresponding to the atrophy seen on ophthalmoscopy, with a surrounding ring of increased AF. *Family A*, *patient III:7*: (**C**) Fundus photographs showing bilateral areas of macular RPE atrophy. (**D**) Fundus AF imaging showing bilateral areas of decreased macular AF corresponding to atrophy seen on ophthalmoscopy, with a surrounding ring of increased AF. *Family A*, *patient III:5*: (**E**) Fundus photographs showing bilateral RPE mottling temporal to the macula. *Family B*, *patient IV:11*: (**F**) Fundus photographs showing bilateral RPE atrophy at the macular and peripapillary region, extending mainly into the inferior retina. (**G**) Fundus AF imaging showing bilateral reduced regions of AF of the RPE. *Family B*, *patient V:10*: (**H**) Fundus photographs showing bilateral foveal RPE mottling. (**I**) Fundus AF showing bilateral macular rings of increased AF, more prominent in the right eye than in the left. *Family*, *B patient III:3*: (**J**) Fundus photographs from a female carrier showing an asymmetrical bilateral macular, peripapillary, and peripheral RPE atrophy, most prominent inferiorly.

DISCUSSION

RPGR mutations, and in particular *RPGR* ORF15 mutations, are a major cause of retinal degeneration,[1–12,21–23] and molecular diagnosis greatly facilitates genetic counseling and advice on prognosis. However, screening ORF15 presents a major technical challenge because of the repetitive and purine-rich nature of the DNA sequence. We have used a cloning strategy to obtain accurate bidirectional full sequence of ORF15 reproducibly which was both cost and time effective. The high level of polymorphism within ORF15, which can often lead to primer-specific amplification failure, is overcome with this method. Once the mutation had been identified within a family, specific primer pairs were then used to amplify and sequence the mutation in other family members. In this study, six unrelated affected males were initially screened for ORF15 mutations, and two of these families were found to harbor ORF15 mutations that segregated with disease. These two families can therefore be described as CORDX1 families. The *RPGR* ORF15 mutations identified in both families were protein-truncating

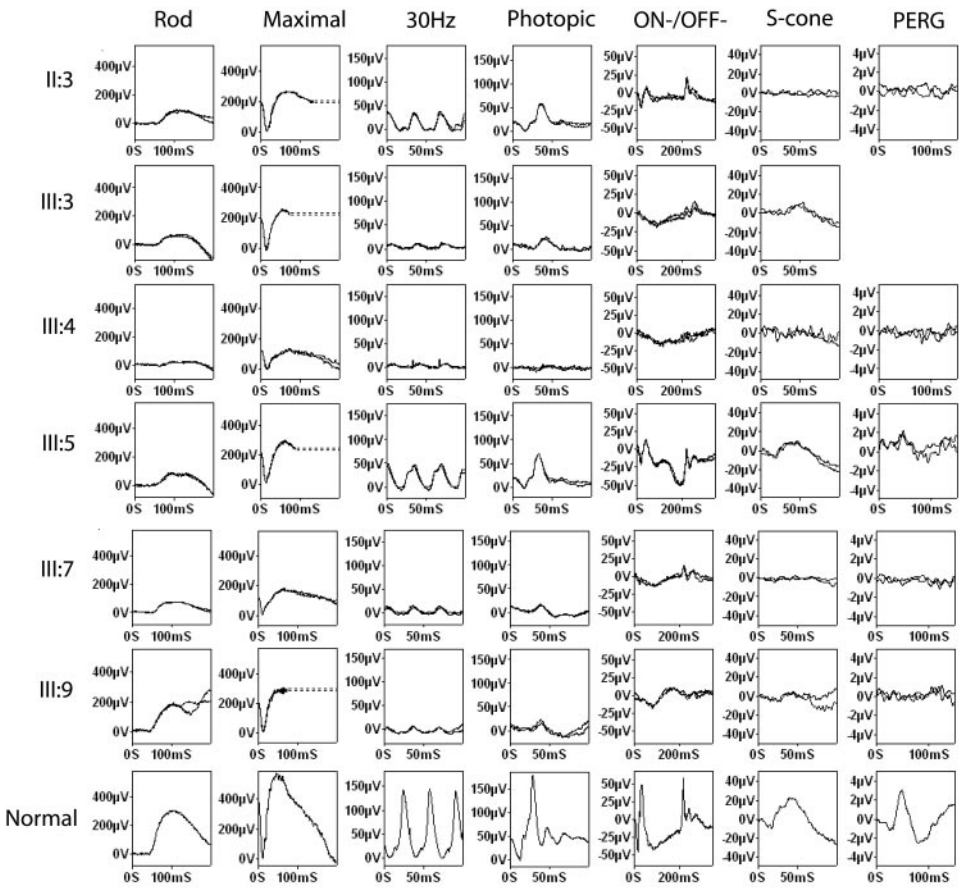

FIGURE 4. Representative electrophysiological traces for family A. II:3 shows rod-specific and maximum ERGs within normal limits for age. Cone single-flash and flicker ERGs show mild to moderate abnormality with delay and amplitude reduction. ON/OFF ERGs and S-cone ERGs were reduced. The PERG was undetectable, in keeping with severe macular dysfunction. III:3 and III:5 showed borderline abnormal rod and maximum ERGs. There was generalized cone dysfunction of moderate severity with mild PERG reduction in III:5. A PERG was not recorded in III:3. III:4 showed rod and maximum ERG reduction of moderate severity, with severe generalized cone dysfunction and undetectable PERG. III:7 and III:9 showed subnormal maximum a-wave response, worse in III:7. Cone ERGs showed moderate to severe abnormality (delayed and reduced) with undetectable PERGs.

nonsense mutations located 3′ to the highly repetitive region of ORF15. It is worth noting that ORF15 mutations reported as a cause of CORDX1 are also at the 3′-end of ORF15; four of the mutations previously described were insertions and deletions resulting in frame shifts, and one was a nonsense mutation.[12,21,22] Similarly, an ORF15 nonsense mutation 3′ to the highly repetitive region was described as a cause of atrophic macular degeneration (although several affected male subjects in that pedigree had electrophysiological data consistent with a cone–rod dystrophy phenotype).[23] Our data strengthen the hypothesis that mutations 3′ to the highly repetitive region cause predominant cone dysfunction. However, exceptions exist to this rule, for example a frame-shift insertion detected 5′ to the repetitive region of ORF15 has been reported in a cone–rod dystrophy pedigree.[28] The significance of the distribution and mutation type is difficult to assess, since the numbers of families with CORDX1 are small in comparison with the large number of XLRP families with ORF15 mutations, and currently there are no functional tests for *RPGR*. Recently, we and others have described *RPGR* mutations causing an XLRP syndrome associated with hearing loss and recurrent respiratory tract infections, highlighting the expanding clinical spectrum of disease associated with *RPGR* mutations.[29–31] Although none of the mutations described occur in ORF15, there was notable inter- and intrafamilial phenotypic variation, with no clear correlation with mutation type.[29–31] Questions are raised about the potential function of RPGR isoforms in different tissues and the consequence of different mutations, and it is hoped that future functional evaluation of this important protein will extend our understanding of mutation hotspots, environmental interplay, and genetic background.

An important finding of this study was the absence of *RPGR* ORF15 mutations in four families with X-linked predominantly cone photoreceptor dysfunction. Two other loci have been reported on the X-chromosome, CORDX2 on Xq27.2-q28[16] and CORDX3 spanning Xp11.4-q13.1,[17] for which the causative genes remain to be identified. We are currently performing linkage analysis and additional clinical evaluation of the remaining pedigrees to identify the X-linked genes that cause cone and cone–rod dystrophies.

The detailed phenotypes described in two unrelated families in which the affected males have premature termination mutations in *RPGR* are consistent with X-linked cone-rod dystrophy (XLCORD). Affected males experience onset of visual symptoms from the second to fourth decade and show progressive deterioration in central vision and subsequently night vision, mild photophobia, and moderate to high myopia. A variation in the severity of the phenotype was seen in family A, with two males being only mildly affected (III:7 and III:9). This is to be expected because of their younger age compared with the other affected males in this family, although it is also possible that this intrafamilial variability of phenotype is due to genetic or environmental modifying factors. The fundoscopic abnormalities were generally restricted to the macular region and ranged from mild RPE disturbance in the early stages to extensive chorioretinal atrophy and pigmentation.

AF imaging allows the visualization of the RPE by taking advantage of the fluorescent properties of lipofuscin.[32,33] To our knowledge, there are no previous data on AF imaging in XLCORD. Older affected male subjects showed decreased AF corresponding to areas of atrophy seen ophthalmoscopically, whereas in family A all five affected males had a ring of increased AF encircling the fovea. This was also clearly observed in the youngest affected male in family B (V:10). One of the five male subjects in family A was asymptomatic with no definite macular disturbance detected on fundoscopy, thereby suggesting that the presence of a parafoveal ring may be used as an early indicator of affected status. This high-density annulus has

TABLE 1. Summary of Clinical Findings for Family A

Patient	Sex	Age (y)	Visual Acuity (OD-OS)	Fundus	AF Imaging	ERG	PERG	Color Vision
II:1	M	74	CF-CF	Bilateral macular atrophy and peripheral retinal degeneration	Bilateral decreased AF corresponding to atrophy seen on ophthalmoscopy with surrounding ring of increased AF	Cone responses more markedly reduced than rod	Absent	Absent
II:3	F	73	6/9-6/36	Bilateral RPE mottling temporal to the macula; areas of myopic chorioretinal atrophy	Normal	Cone responses more markedly reduced than rod	Absent	Normal
III:1	F	41	6/4-6/4	Bilateral RPE mottling temporal to the macula	Normal	Normal	Normal	Normal
III:2	F	38	6/4-6/4	Bilateral RPE mottling temporal to the macula	Normal	Normal	Normal	Normal
III:3	M	51	CF-CF	Bilateral macular atrophy with surrounding RPE changes	Bilateral decreased AF corresponding to atrophy, with surrounding ring of increased AF	Cone responses more markedly reduced than rod	Absent	Absent
III:4	M	48	CF-CF	Bilateral macular atrophy and pigmentation (Fig. 3A)	Bilateral decreased AF corresponding to atrophy, with surrounding ring of increased AF (Fig. 3B)	Cone responses more markedly reduced than rod	Absent	Absent
III:5	F	50	6/9-6/9	Bilateral RPE mottling temporal to the macula (Fig. 3E)	Normal	Cone responses more markedly reduced than rod	Reduced	Normal
III:7	M	40	6/5-6/5	Bilateral macular RPE atrophy (Fig. 3C)	Bilateral decreased AF corresponding to notable areas of atrophy with a surrounding ring of increased AF (Fig. 3D)	Cone responses more markedly reduced than rod	Absent	Absent
III:8	F	38	6/5-6/5	Normal	Normal	Normal	Normal	Normal
III:9	M	37	6/6-6/6	No definite abnormality	Bilateral decreased central macular AF with a surrounding ring of increased AF	Cone responses more markedly reduced than rod	Absent	Absent

CF, counting fingers; NP, not performed.

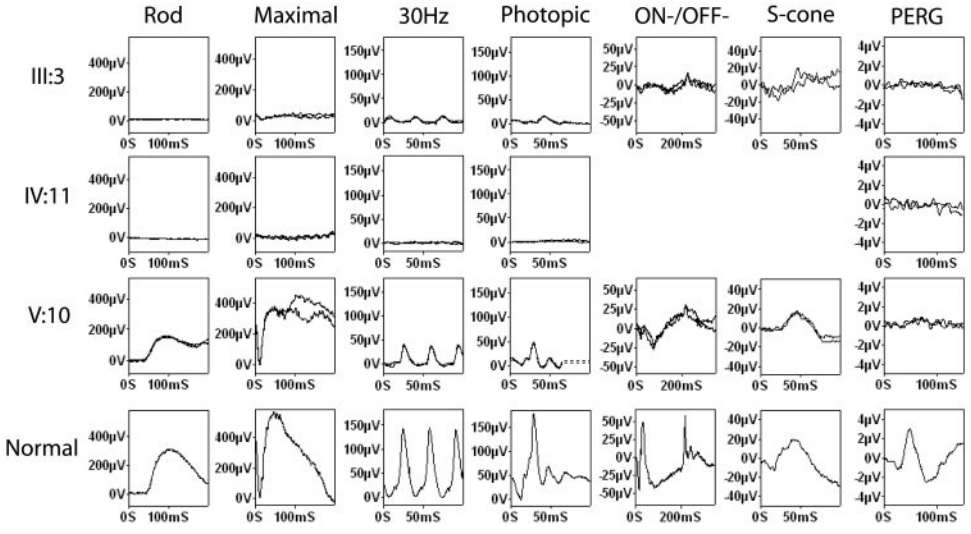

FIGURE 5. Representative electrophysiological traces for family B. III:3 showed severe generalized loss of retinal function, with the rod system more affected. The PERG was undetectable, in keeping with severe macular involvement. IV:2 showed no detectable ERG responses. V:10 showed normal rod and maximum responses. Cone ERGs were markedly reduced and mildly delayed, with S-cone ERGs showing loss of the early L/M-cone component but preservation of the later, S-cone specific component. PERG showed some residual activity but are markedly abnormal in keeping with moderate to severe macular involvement.

TABLE 2. Summary of Clinical Findings for Family B

Patient	Sex	Age (y)	Visual Acuity (OD-OS)	Fundus	AF Imaging	ERG	PERG	Color Vision
IV:3	M	73	6/60-2/60	Bilateral macular and peripapillary atrophy; areas of myopic chorioretinal atrophy	NP	Cone responses more markedly reduced than rod	NP	NP
V:1	M	50	3/60-3/36	Bilateral RPE atrophy in the posterior pole, around the optic disc and inferior sector	NP	Cone responses more markedly reduced than rod	NP	Absent
III:3	F	70	CF-6/12	Bilateral macular and peripapillary atrophy, asymmetric between both eyes, with peripheral involvement and sharp demarcation (Fig. 3J)	Bilateral decreased AF corresponding to notable areas of atrophy with surrounding increased AF	Generalized cone and rod dysfunction, right eye more affected than left eye	Absent right; reduced left	NP
IV:11	M	44	1/36−1-3/36+1	Bilateral macular and peripapillary RPE atrophy; some pigment migration in the periphery (Fig. 3F)	Bilateral decreased AF corresponding to Notable areas of atrophy with surrounding increased AF (Fig. 3G)	Generalized cone and rod dysfunction with residual activity in the scotopic maximum ERG	Absent	Absent
V:10	M	22	6/6-6/12	Mottling RPE macula; abnormal reflex inferiorly (Fig. 3H)	Parafoveal ring of increased AF (Fig. 3I)	General loss of cone system function; minimal rod involvement	Reduced	Absent

CF, counting fingers; NP, not performed.

also been reported in the autosomal dominant cone–rod dystrophy, CORD7.[34] It has been proposed that there is an accumulation of autofluorescent material before photoreceptor cell death. This is supported by the histologic demonstration of a reduction in the number of photoreceptors in the presence of and increased quantity of lipofuscin in the RPE in age-related macular disease.[35,36] These findings suggest that the ring of increased AF in our patients may represent the front of advancing concentric photoreceptor cell loss. Reduced rod sensitivity has been demonstrated across the similar-appearing ring of increased AF that can occur in retinitis pigmentosa, and a similar mechanism has been proposed.[37] It has also been suggested that this hyperfluorescent annulus may correspond to the "rod ring" that surrounds the fovea; an area of high rod photoreceptor density.[38] Previous studies of XLCORD pedigrees have reported variable clinical, electrophysiological, and psychophysical findings in carrier females, with a lack of consistent abnormalities between subjects.[15,18–20] In our family A, the younger carrier females were asymptomatic and had normal electrophysiological and psychophysical testing. The two older carrier females had reduced central and peripheral retinal function, consistent with a cone–rod pattern of dysfunction with marked bilateral macular involvement. Another consistent finding in all carrier females in family A was a mottling of the RPE temporal to the macula, suggesting that this may be an indicator of carrier status in this family. Unlike these cone–rod dystrophy carrier females, who were found to have normal AF imaging, a recent study of carrier females of rod–cone dystrophy associated with *RPGR* mutations has described an abnormal AF pattern in 9 of 11 carriers investigated,[38] suggesting further phenotypic differences between XLCORD and XLRP carriers. In family B, obligate female carriers and two affected males had a golden tapetal retinal reflex. No tapetal sheen was observed in individuals from family A. A tapetallike retinal sheen has been variously described in affected male and carrier females of XLCORD.[15,38] One of the two carrier females tested in family B had electrophysiological evidence of bilateral generalized retinal dysfunction affecting both cone and rod photoreceptors.

We have described the detailed phenotype of two XLCORD families with novel disease causing *RPGR* ORF15 mutations. The clinical findings are consistent with previous reports of CORDX1 phenotypes associated with mutations in *RPGR* ORF15. Important novel AF data are described that suggest that, in addition to electrophysiology, AF imaging may be helpful in establishing affected status at an early asymptomatic stage. We have also identified a consistent retinal phenotype in both of our families that will assist in clinically identifying carrier females. Our cloning strategy for ORF15 facilitated comprehensive sequence analysis of ORF15 in patients with X-linked retinal degeneration. This method is recommended as a potential initial strategy for diagnostics. The data add to the genotype and phenotype descriptions for CORDX1 and highlight the lack of ORF15 mutations in other families, suggesting that ORF15 may not be the most common cause of X-linked cone-rod dystrophy.

Acknowledgments

The authors thank the patients who kindly agreed to take part in the study and Hannah Smithson, MD, for help with the psychophysical testing.

References

1. Meindl A, Dry K, Herrmann K, et al. A gene (RPGR) with homology to the RCC1 guanine nucleotide exchange factor is mutated in X-linked retinitis pigmentosa (RP3). *Nat Genet.* 1996;13:35–42.
2. Roepman R, van Duijnhoven G, Rosenberg T, et al. Positional cloning of the gene for X-linked retinitis pigmentosa 3: homology with the guanine-nucleotide-exchange factor RCC1. *Hum Mol Genet.* 1996;5:1035–1041.
3. Vervoort R, Lennon A, Bird AC, et al. Mutational hot spot within a new RPGR exon in X-linked retinitis pigmentosa. *Nat Genet.* 2000; 25:462–466.

4. Buraczynska M, Wu W, Fujita R, et al. Spectrum of mutations in the RPGR gene that are identified in 20% of families with X-linked retinitis pigmentosa. *Am J Hum Genet*. 1997;61:1287–1292.
5. Zito I, Thiselton DL, Gorin MB, et al. Identification of novel RPGR (retinitis pigmentosa GTPase regulator) mutations in a subset of X-linked retinitis pigmentosa families segregating with the RP3 locus. *Hum Genet*. 1999;105:57–62.
6. Miano MG, Testa F, Strazzullo M, et al. Mutation analysis of the RPGR gene reveals novel mutations in south European patients with X-linked retinitis pigmentosa. *Eur J Hum Genet*. 1999;7:687–694.
7. Zito I, Gorin MB, Plant C, Bird AC, Bhattacharya SS, Hardcastle AJ. Novel mutations of the RPGR gene in RP3 families. *Hum Mutat*. 2000;15:386.
8. Rozet JM, Perrault I, Gigarel N, et al. Dominant X linked retinitis pigmentosa is frequently accounted for by truncating mutations in exon ORF15 of the RPGR gene. *J Med Genet*. 2002;39:284–285.
9. Breuer DK, Yashar BM, Filippova E, et al. A comprehensive mutation analysis of RP2 and RPGR in a North American cohort of families with X-linked retinitis pigmentosa. *Am J Hum Genet*. 2002;70:1545–1554.
10. Pusch CM, Broghammer M, Jurklies B, Besch D, Jacobi FK. Ten novel ORF15 mutations confirm mutational hot spot in the RPGR gene in European patients with X-linked retinitis pigmentosa. *Hum Mutat*. 2002;20:405.
11. Bader I, Brandau O, Achatz H, et al. X-linked retinitis pigmentosa: RPGR mutations in most families with definite X linkage and clustering of mutations in a short sequence stretch of exon ORF15. *Invest Ophthalmol Vis Sci.* 2003;44:1458–1463.
12. Sharon D, Sandberg MA, Rabe VW, Stillberger M, Dryja TP, Berson EL. RP2 and RPGR mutations and clinical correlations in patients with X-linked retinitis pigmentosa. *Am J Hum Genet*. 2003;73:1131–1146.
13. Bird AC. X-linked retinitis pigmentosa. *Br J Ophthalmol*. 1975;59:177–199.
14. Fishman GA. Retinitis pigmentosa: visual loss. *Arch Ophthalmol*. 1978;96:1185–1188.
15. Hong H.-K, Ferrell RE, Gorin MB. Clinical diversity and chromosomal localization of X-linked cone dystrophy (COD1). *Am J Hum Genet*. 1994;55:1173–1181.
16. Bergen AA, Pinckers AJ. Localization of a novel X-linked progressive cone dystrophy gene to Xq27: evidence for genetic heterogeneity. *Am J Hum Genet*. 1997;60:1468–1473.
17. Jalkanen R, Demirci FY, Tyynismaa H, et al. A new genetic locus for X linked progressive cone-rod dystrophy. *J Med Genet*. 2003;40:418–423.
18. Jacobson DM, Thompson S, Bartley JA. X-linked progressive cone dystrophy: clinical characteristics of affected males and female carriers. *Ophthalmology*. 1989;96:885–895.
19. Brown J Jr, Kimura AE, Gorin MB. Clinical and electroretinographic findings of female carriers and affected males in a progressive X-linked cone-rod dystrophy (COD-1) pedigree. *Ophthalmology*. 2000;107:1104–1110.
20. Mantyjarvi M, Nurmenniemi P, Partanen J, et al. Clinical features and a follow-up study in a family with X-linked progressive cone-rod dystrophy. *Acta Ophthalmol Scand*. 2001;79:359–365.
21. Demirci FY, Rigatti BW, Wen G, et al. X-linked cone-rod dystrophy (locus COD1): identification of mutations in RPGR exon ORF15. *Am J Hum Genet*. 2002;70:1049–1053.
22. Yang Z, Peachey NS, Moshfeghi DM, et al. Mutations in the RPGR gene cause X-linked cone dystrophy. *Hum Mol Genet*. 2002;11:605–611.
23. Ayyagari R, Demirci FY, Liu J, et al. X-linked recessive atrophic macular degeneration from RPGR mutation. *Genomics*. 2002;80:166–171.
24. Marmor MF, Zrenner E. Standard for clinical electro-oculography. International Society for Clinical Electrophysiology of Vision. *Arch Ophthalmol*. 1993;111:601–604.
25. Marmor MF, Zrenner E. Standard for clinical electroretinography (1999 update). *Doc Ophthalmol*. 1998;97:143–156.
26. Bach M, Hawlina M, Holder GE, et al. Standard for pattern electroretinography: International Society for Clinical Electrophysiology of Vision. *Doc Ophthalmol*. 2000;101:11–18.
27. Keunen JE, van Everdingen JA, Went LN, Oosterhuis JA, van Norren D. Color matching and foveal densitometry in patients and carriers of an X-linked progressive cone dystrophy. *Arch Ophthalmol*. 1990;108:1713–1719.
28. Mears AJ, Hiriyanna S, Vervoort R, et al. Remapping of the RP15 locus for X-linked cone-rod degeneration to Xp11.4-p21.1, and identification of a de novo insertion in the RPGR exon ORF15. *Am J Hum Genet*. 2000;67:1000–1003.
29. Zito I, Downes SM, Patel RJ, et al. RPGR mutation associated with retinitis pigmentosa, impaired hearing, and sinorespiratory infections. *J Med Genet*. 2003;40:609–615.
30. Iannaccone A, Breuer DK, Wang XF, et al. Clinical and immunohistochemical evidence for an X linked retinitis pigmentosa syndrome with recurrent infections and hearing loss in association with an RPGR mutation. *J Med Genet*. 2003;40:E118.
31. Koenekoop RK, Loyer M, Hand CK, et al. Novel RPGR mutations with distinct retinitis pigmentosa phenotypes in French-Canadian families. *Am J Ophthalmol*. 2003;136:678–687.
32. von Rückmann A, Fitzke FW, Bird AC. Distribution of fundus autofluorescence with a scanning laser ophthalmoscope. *Br J Ophthalmol*. 1995;79:407–412.
33. von Rückmann A, Fitzke FW, Bird AC. Distribution of pigment epithelium autofluorescence in retinal disease state recorded *in vivo* and its change over time. *Graefes Arch Clin Exp Ophthalmol*. 1999;237:1–9.
34. Michaelides M, Holder GE, Hunt DM, et al. A detailed study of the phenotype of an autosomal dominant cone-rod dystrophy (CORD7) associated with mutation in the gene for RIM1. *Br J Ophthalmol*. 2005;89:198–206.
35. von Rückmann A, Fitzke FW, Bird AC. Fundus autofluorescence in age related macular disease imaged with a scanning laser ophthalmoscope. *Invest Ophthalmol Vis Sci*. 1997;38:478–486.
36. Dorey CK, Wu G, Ebenstein D, Garsd A, Weiter JJ. Cell loss in the ageing retina: relationship to lipofuscin accumulation and macular degeneration. *Invest Ophthalmol Vis Sci*. 1989;30:1691–1699.
37. Robson AG, El-Amir A, Bailey C, et al. Pattern ERG correlates of abnormal fundus autofluorescence in patients with retinitis pigmentosa and normal visual acuity. *Invest Ophthalmol Vis Sci*. 2003;44:3544–3550.
38. Wegscheider E, Preising MN, Lorenz B. Fundus autofluorescence in carriers of X-linked recessive retinitis pigmentosa associated with mutations in RPGR, and correlation with electrophysiological and psychophysical data. *Graefes Arch Clin Exp Ophthalmol*. 2004;242:501–511.